Model Predictive Control of a Direct Wave Energy Converter Constrained by the Electrical Chain using an Energetic Approach

Thibaut Kovaltchouk, François Rongère, Muriel Primot, Judicael Aubry, Hamid Ben Ahmed, Bernard Multon

▶ **To cite this version:**

Thibaut Kovaltchouk, François Rongère, Muriel Primot, Judicael Aubry, Hamid Ben Ahmed, et al.. Model Predictive Control of a Direct Wave Energy Converter Constrained by the Electrical Chain using an Energetic Approach. European Wave and Tidal Energy Conference 2015, Sep 2015, Nantes, France. hal-01195536

HAL Id: hal-01195536
https://hal.science/hal-01195536

Submitted on 7 Sep 2015

HAL is a multi-disciplinary open access archive for the deposit and dissemination of scientific research documents, whether they are published or not. The documents may come from teaching and research institutions in France or abroad, or from public or private research centers.

L'archive ouverte pluridisciplinaire **HAL**, est destinée au dépôt et à la diffusion de documents scientifiques de niveau recherche, publiés ou non, émanant des établissements d'enseignement et de recherche français ou étrangers, des laboratoires publics ou privés.

Model Predictive Control of a Direct Wave Energy Converter Constrained by the Electrical Chain using an Energetic Approach

Thibaut Kovaltchouk*†, François Rongère‡, Muriel Primot†,
Judicaël Aubry§, Hamid Ben Ahmed* and Bernard Multon*
*SATIE CNRS UMR8029, ENS Rennes, UEB, Avenue Robert Schuman, Bruz, France
†IRCCyN, CNRS UMR6597, LUNAM, Ecole Centrale de Nantes, Nantes, France
‡LHEEA, CNRS UMR6598, LUNAM, Ecole Centrale de Nantes, Nantes, France
§Mechatronics team, ESTACA, CERIE, Laval, France

***Abstract*—The control strategy for Direct Wave Energy Converters (DWEC) is often discussed without taking into account the physical limitations of electric Power Take-Off (PTO) system. This inappropriate modelling assumption leads to a non-realistic or a bad use of the electric systems, that leads to a failure to minimize the global "per-kWh" system cost. We propose here a Model Predictive Control (MPC) that takes into account the main limits of an electrical chain: maximum force, maximum power and a simplified loss model of the electrical chain. To compare this optimal control with other strategies, we introduce the notions of control, electric and global energy efficiencies. Furthermore, we use an original energy representation used to value the state at the end of the MPC horizon. Finally, we make several sensitivity study on the constraint limits for an economical pre-sizing of the electrical chain.**

***Index Terms*—Optimal Control, Model Predictive Control, Direct Wave Energy Converter, Pontryagin's Maximum Principle, Direct Multiple Shooting Method, Energetic Model, Electric Power Take-Off**

NOMENCLATURE

A	State matrix (6×6) of the buoy system
A_{rad}	State matrix (4×4) of the radiation system
a_∞	Added mass of the buoy (radiation effect) [kg]
$b()$	Barrier function
B_{rad}	Input matrix (4×1) of the radiation system
B_1	Control matrix (6×1) of the buoy: system $\begin{bmatrix}0 & -(m+a_\infty)^{-1} & (0)\end{bmatrix}^T$
B_2	Perturbation matrix (6×1) of the buoy system: $\begin{bmatrix}0 & +(m+a_\infty)^{-1} & (0)\end{bmatrix}^T$
C	Output matrix (1×6) of the buoy system
c_{loss}	Electrical loss coefficient [W·N^{-2}]
$\tilde{c}_{loss}$	Loss coefficient used in the control problem [W·N^{-2}]
C_{rad}	Output matrix (1×4) of the radiation system
E_{Mech}	Mechanical energy stored in the system [J]
$f()$	Dynamic function of the buoy system $\dot{x} = f(x,u,t)$
f_{exc}	Wave excitation force, time domain [N]
F_{exc}	Wave excitation force, Laplace domain [N]
F_{Max}	Maximum Power Take-Off force [N]
f_{PTO}	Power Take-Off force, time domain [N]
F_{PTO}	Power Take-Off force, Laplace domain [N]
H	Hamiltonian of the control problem [W·kg^{-1}]
$H_{rad}(s)$	Impulse radiation response, Laplace domain [kg·s^{-1}]
H_s	Significant height of the sea state [m]
J	Objective function of the control problem [J·kg^{-1}]
k_{hs}	Hydrostatic stiffness of the buoy [kg·s^{-2}]
L	Lagrangian of the control problem [W·kg^{-1}]
m	Mass of the buoy [kg]
p	Costate vector (1×6)
P	Positive definite matrix: $E_{Mech} = x^T\ P\ x$
P_{Loss}	Mechanical power lost in the system [W]
P_{exc}	Excitation power $f_{exc}\dot{z}$ [W]
P_{Max}	Maximum Power Take-Off power [W]
P_{PTO}	Power Take-Off mechanical power $f_{PTO}\dot{z}$ [W]
p_2	Second element of p
Q	Positive definite matrix: $P_{Loss} = x^T\ Q\ x$
T_p	Peak period of the sea state [s]
u	Control input of the buoy system: $u = f_{PTO}$
w	Perturbation input of the buoy system: $w = f_{exc}$
x	State vector (6×1) of the buoy system: $\begin{bmatrix}z & \dot{z} & x_{rad}\end{bmatrix}^T$
x_{rad}	State vector (4×1) of the radiation system
x_2	Second element of x: $\dot{z}$

© 2015 European Wave and Tidal Energy Conference 2015. Personal use of this material is permitted. Permission from European Wave and Tidal Energy Conference (EWTEC) must be obtained for all other uses, including reprinting/republishing this material for advertising or promotional purposes, collecting new collected works for resale or redistribution to servers or lists, or reuse of any copyrighted component of this work in other works.
Kovaltchouk, Thibaut; Rongere, François; Primot, Muriel; Aubry, Judicael; Ben Ahmed, Hamid; Multon, Bernard, "Model Predictive Control of a Direct Wave Energy Converter Constrained by the Electrical Chain using an Energetic Approach," European Wave and Tidal Energy Conference, 2015, Nantes, pp.1,10, 6-11 September 2015
ISSN 2309-1983, paper ID: 07D3-1

y	Output of the buoy system: $y = \dot{z}$
z	Vertical position of the buoy, time domain [m]
Z	Vertical position of the buoy, Laplace domain [m]
ϵ	Parameter of the barrier function $b()$
η_C	Control energy efficiency
η_E	Electrical energy efficiency
$\psi()$	Weight of the final state [J·kg^{-1}]

I. Introduction

Direct Wave Energy Converters (DWEC) (or Wave Activated Bodies), with electric Power Take-Off (PTO) are one of the most direct and flexible way to convert wave energy into electrical energy, because there is no buffer between the waves and the electrical chain contrary to Oscillating Water Column, Overtopping device or Wave Energy Converters with mechanical or hydropneumatic transmission. They may make use of mechanical transmission (gear box, rack and pinion, etc) or may not (direct drive). They lead to the possibility of higher efficiency and reliability, yet feature higher power fluctuations in the grid than WEC with hydraulic or mechanical storage systems. The test case considered here to represent DWECs is a heaving buoy, but the method can be reused for all DWEC with electric PTO.

In order to minimize the per-kWh cost of this technology, the global efficiency from wave to wire must increase, while limiting the size of the electric PTO (classically an electrical machine with an active rectifier).

Control design, however, must take into account the main limitations of an electric PTO, i.e.: power limitation, force or torque limitation and losses in the electric chain. But the problem is often seen as decoupled. Thus, two types of papers classically deal with control strategies in DWEC: the theoretical optimization of control with no or very little considerations for the feasibility limitations [1]–[3]; and optimization using a given electric system [4]. Some studies take into account only losses [5], [6], or power limitation [7], or force limitation [8]. To the best of our knowledge, it is the first time a Model Predictive Control of a Wave Energy Converter takes into account all the main constraints of an electrical chain.

Furthermore, only a few papers have dealt with the coupling between control strategy and sizing [9].

II. Models

A. Dynamic Model of the Buoy

The considered buoy is 10 meters in diameter and 15 meters in height. It is illustrated in figure 1 and its physical parameters are given in TABLE I.

The model chosen is linear within the framework of linear potential theory (small displacement) and under the hypotheses of infinite water depth. This model of the buoy takes into account the hydrostatic effect (with the hydrostatic stiffness k_{hs}), the radiation effect (with the added mass a_∞, the radiation vector state x_{rad} and the matrices A_{rad}, B_{rad} and

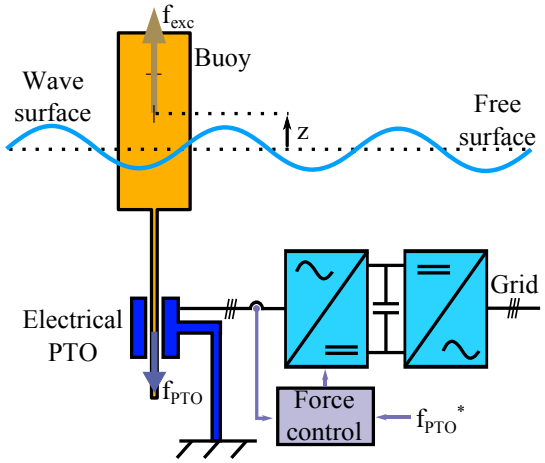

Fig. 1. Simple 1-degree-of-freedom test-case used as an example for the illustration of the MPC

C_{rad}) and the excitation effect from the waves f_{exc}, as for example, in [10] [11]:

$$(m + a_\infty)\ \ddot{z} + C_{rad}\ x_{rad} + k_{hs}\ z = f_{exc} - f_{PTO} \quad (1)$$

$$\dot{x}_{rad} = A_{rad} x_{rad} + B_{rad} \dot{z} \quad (2)$$

with z, the vertical position of the buoy, M, the buoy mass, and f_{PTO}, the controllable force from the electrical Power Take-Off.

These equations can be rewritten in the Laplace domain (with s the Laplace variable) and Z, F_{PTO} and F_{exc}, the Laplace transformations of z, f_{PTO} and f_{exc}:

$$F_{exc} - F_{PTO} = Z\left((m + a_\infty)s^2 + H_{rad}(s)s + k_{hs}\right) \quad (3)$$

$$H_{rad}(s) = C_{rad}\ (sI - A_{rad})^{-1}\ B_{rad} \quad (4)$$

with I, the identity matrix with the same size as A_{rad} (4 by 4 in our case) and $H_{rad}(s)$ the Laplace transformation of the impulse radiation response.

The inertia, stiffness and radiation transfer function are given in TABLE I. The parameters have been computed in the AQUAPLUS seakeeping code for hydrodynamics simulations [12].

TABLE I
Parameters of the hydrodynamic buoy model

m (kg)	a_∞ (kg)	k_{hs} (kg·s^{-2})
$772 \cdot 10^3$	$247 \cdot 10^3$	$758 \cdot 10^3$

$$H_{rad}(s) = C_{rad}(sI - A_{rad})^{-1}B_{rad}\ (\text{kg·s}^{-1}) = \frac{13.4s^3 + 19.3s^2 + 5.87s}{s^4 + 1.56s^3 + 1.51s^2 + 0.714s + 0.156} \cdot 10^3$$

We will use $x = [z\ \dot{z}\ x_{rad}]^T$ as the system state vector. We consider that we can control the force of the PTO $u = f_{PTO}$ and the excitation is considered as a perturbation $w = f_{exc}$:

$$\dot{x} = Ax + B_1 u + B_2 w(t) = f(x, u, t) \quad (5)$$

$$y = Cx = \dot{z} \quad (6)$$

with A, B_1, B_2 and C, respectively the state, the control, the perturbation and the output matrices of the buoy system that takes as inputs forces (u and w) and that gives the speed of the buoy as an output (y). The speed was chosen as the only output because this variable is linked with the excitation power $P_{exc} = \dot{z}\ f_{exc}$ and the PTO mechanical power $P_{PTO} = \dot{z}\ f_{PTO}$. It has been verified that this system is controllable and observable.

A JONSWAP spectrum is used to compute the excitation force [13]. The frequency spreading parameter γ was chosen equal to 3. The excitation force time series (corresponding to wave data) is generated by summing monochromatic excitation with randomly chosen initial phases. In our case, this configuration is similar to the solution of a reconstructed wave elevation with a random phase, as presented in [14].

This dynamic equation is solved using the Heun's ordinary differential equation solver (explicit trapezoidal rule) with a fixed time step of 0.1 s.

B. Energetic Model of the Buoy

Because the model is linear and passive, there exist a couple of two positive semidefinite matrices P and Q that defines the mechanical energy stored in the system and the power loss with the radiation effects:

$$E_{Mech} = x^T\ P\ x \tag{7}$$
$$P_{Loss} = x^T\ Q\ x \tag{8}$$

These two terms respect the conservation of energy with the following equation:

$$\dot{E}_{Mech} = P_{exc} - P_{PTO} - P_{Loss} \tag{9}$$

with the excitation power P_{exc} and the PTO mechanical power P_{PTO}.

In order to find these two equations, we need to solve the following semidefinite programming problem, for example with CVX [15]:

$$B_2^T\ (2\ P) = C \tag{10}$$
$$A^T\ P + P\ A + Q = 0 \tag{11}$$

Fig. 2 illustrates a decay test used to test the accuracy of this energetic model: without excitation and harvesting, the time derivative of the mechanical energy corresponds exactly to the mechanical loss $x^T\ Q\ x$. Such a model gives information on power flows that is essential for energy conversion studies.

C. Model of the Electrical Chain

The electrical chain is simplified by considering two constraints and one term of losses.

The absolute value of the force is limited by a maximum value F_{Max} mainly due to the limitation of the electrical machine (electromagnetic converter) and the absolute value of the power is limited by a maximum value P_{Max} due to the limitation of the active rectifier (power electronics converter).

Finally, we subtract from the mechanical power of the PTO system, electric losses assumed to be proportional to the square

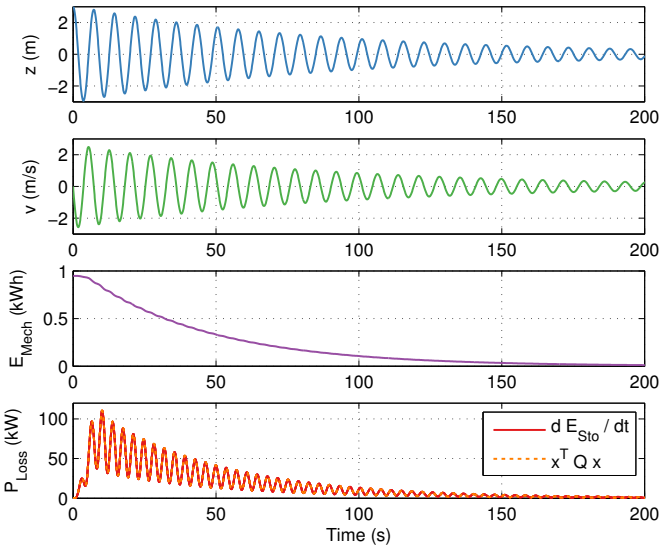

Fig. 2. Decay test from a height of 3 meters: position, speed, energy and power loss vs. time

value of the force. More precise model could take into account copper and iron losses in the electrical machine as well as conduction and switching losses in the active rectifier [9].

This model can be summarized by figure 3 or these three equations:

$$|f_{PTO}| \leq F_{max} \tag{12}$$
$$|f_{PTO} \cdot \dot{z}| \leq P_{max} \tag{13}$$
$$P_{Grid} = f_{PTO} \cdot \dot{z} - c_{loss}\ f_{PTO}^2 \tag{14}$$

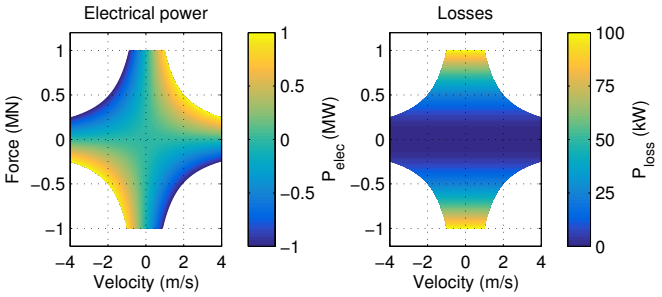

Fig. 3. Electrical power and electrical loss power as a function of Buoy velocity $\dot{z}$ and Power Take-Off force f_{PTO} with F_{max} =1 MN, P_{max} =1 MW and c_{loss} =0.1 MW/MN^2

D. Energy Efficiency

Control efficiency is defined with the maximal theoretical recoverable power $\overline{P_{Wave}}$ as in [11]. With the wave spectrum used in our case, we have:

$$\overline{P_{Wave}} \approx 103\ H_s^2\ T_p^3 \tag{15}$$

with H_s and T_p, respectively the significant height and the peak period of the sea state considered.

So we define the energy efficiency of the control η_C and of the electrical chain η_E as:

$$\eta_C = \frac{\overline{P_{PTO}}}{\overline{P_{Wave}}} \tag{16}$$

$$\eta_E = \frac{\overline{P_{Grid}}}{\overline{P_{PTO}}} \tag{17}$$

$$\eta_C\ \eta_E = \frac{\overline{P_{Grid}}}{\overline{P_{Wave}}} \tag{18}$$

III. Model Predictive Control with Pontryagin's Maximum Principle

We want to use the Pontryagin's maximum principle [16] to perform a Model Predictive Control for an optimal energy harvesting. This is achieved by optimizing on a finite time horizon T_h. So we need observation and prediction, as we can see in Fig.4 that represent the global interactions between the main elements of the device.

We will suppose here a perfect knowledge of the state of the system x at the decision instant t_0 and a perfect knowledge of the excitation force from t_0 to $t_0 + T_h$.

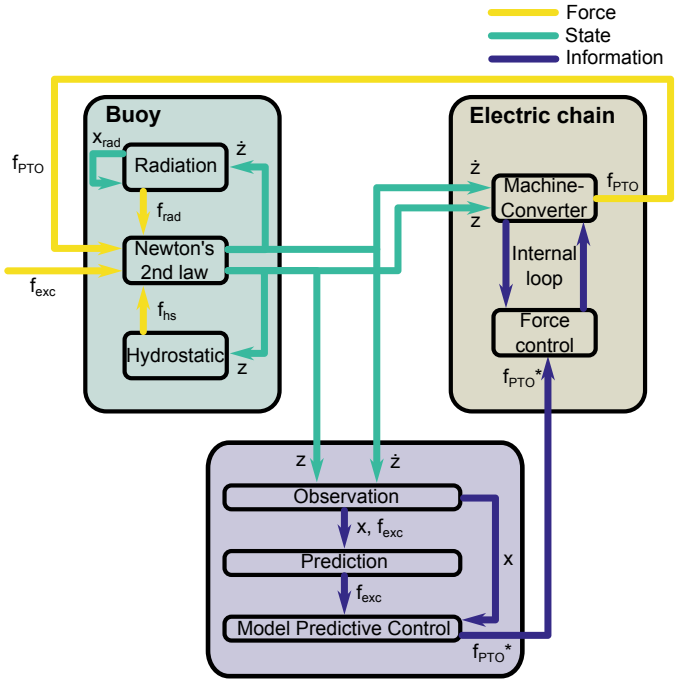

Fig. 4. Interactions between buoy, electrical chain and control

Actually, to have such information, we need observation and prediction, and these can't be perfect.

A. Use of a Barrier Function for the Power Constraint

The problem is to maximize, under a force and power constraints, the average value of the Lagrangian L:

$$L(x,u) = \frac{1}{m + a_\infty}\left(f_{PTO}\cdot\dot{z} - \tilde{c}_{loss}\cdot f_{PTO}^2\right) \tag{19}$$

$$\text{s.t. } |f_{PTO}| \leq F_{max} \tag{20}$$

$$|f_{PTO}\cdot\dot{z}| \leq P_{max} \tag{21}$$

Here, we don't use exactly the electrical power, but an approximation of the electrical power with a loss coefficient $\tilde{c}_{loss}$ that can be different from c_{loss}. Let's notice that the inertia term $(m + a_\infty)$, does not change the problem and is here for dimension issue.

The power constraint is a mixed constraint state-control which complicates the use of the Pontryagin's maximum principle [17]. In order to avoid this difficulty, we change the problem by using a barrier function b:

$$L(x,u) = \frac{1}{m + a_\infty}\left(f_{PTO}\cdot\dot{z} - \tilde{c}_{loss}\cdot f_{PTO}^2 - P_{max}\cdot b\left(\frac{f_{PTO}\cdot\dot{z}}{P_{max}}\right)\right) \tag{22}$$

$$\text{s.t. } |f_{PTO}| \leq F_{max} \tag{23}$$

where the barrier function b is defined by:

$$b(a) = \begin{cases} 0 & \text{if} \quad |a| \leq 1-\epsilon \\ 0.5\left(\dfrac{|a| - (1-\epsilon)}{\epsilon}\right)^2 & \text{if} \quad |a| > 1-\epsilon \end{cases} \tag{24}$$

We will need in the future the derivative function b':

$$b'(a) = \begin{cases} 0 & \text{if} \quad |a| \leq 1-\epsilon \\ \dfrac{\text{sign}(a)}{\epsilon^2}\left(|a| - (1-\epsilon)\right) & \text{if} \quad |a| > 1-\epsilon \end{cases} \tag{25}$$

Let's notice that b' is a monotonically decreasing function and that $b'(a) = sign(a)\cdot b'\left(|a|\right)$.

Graphical representations of this barrier function are shown in figure 5 for different value of ϵ.

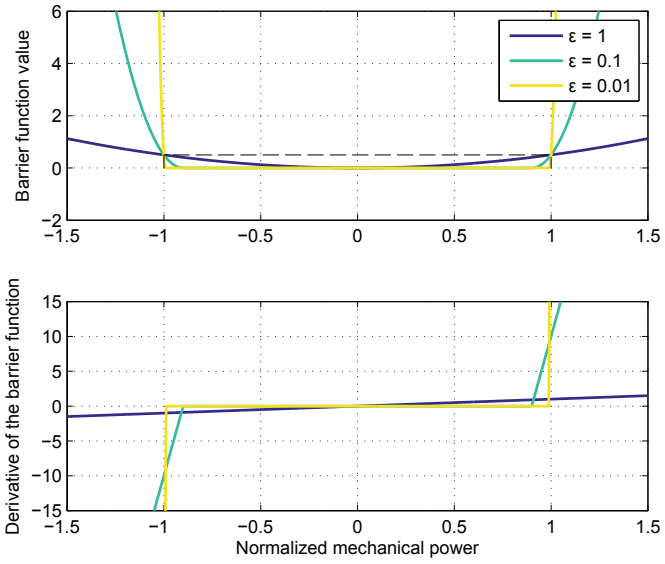

Fig. 5. Barrier function and its derivative function used for the power constraint with $\epsilon = 1$, $\epsilon = 0.1$ and $\epsilon = 0.01$

B. Objective Function

The objective function to maximize is J defined at each time t_0 by:

$$J(t_0) = \int_{t_0}^{t_0+T_h} L(x,u)\,\mathrm{d}t + \Psi(x(t_0+T_h)) \tag{26}$$

The function Ψ gives a weight to the final horizon state. Without such weight, the control naturally tends to convert all the energy stored by the DWEC at the end of the horizon. We will here use a portion α of the mechanical energy E_{Mech} that can be used after the horizon:

$$\Psi(x) = \frac{1}{m+a_\infty} \cdot \alpha \cdot E_{Mech}(x) \tag{27}$$

$$= \frac{1}{m+a_\infty} \cdot \alpha \cdot x^T\ P\ x \tag{28}$$

With $\alpha = 0$, we consider that this energy has no value, and with $\alpha = 1$, we consider that this energy has the same value as the energy converted during the time horizon.

C. Hamiltonian and Dynamic of the Costate vector

The Hamiltonian is defined by:

$$H = p^T f(x,u,t) + L(x,u) \tag{29}$$

with p, the costate vector, of the same size as the state vector.

The dynamic of this costate vector p is:

$$\dot{p} = -\frac{\partial H}{\partial x} \tag{30}$$

$$= -A^T p + B_1\ f_{PTO}\left[1 - b'\left(\frac{\dot{z}\cdot f_{PTO}}{P_{Max}}\right)\right] \tag{31}$$

And the final costate value must satisfy the following transversal condition:

$$p(t_0+T_h) = \frac{\partial \Psi}{\partial x} \tag{32}$$

$$= \frac{1}{m+a_\infty} \cdot \alpha \cdot 2\ P\ x(t_0+T_h) \tag{33}$$

D. Maximization of the Hamiltonian

The Pontryagin's maximum principle states that the maximization of the function J is obtained only if the control f_{PTO} maximizes the Hamiltonian H at all instant t.

There are two possibilities:

- The maximum of the Hamiltonian is in the admissible control interval ($|f_{PTO}| \leq F_{max}$);
- The maximum of the Hamiltonian is outside the admissible control interval: $f_{PTO} = \text{sign}\left(\frac{\partial H}{\partial f_{PTO}}\right) F_{max}$.

We begin by making the hypothesis that we are in the first case. To find the extremum of the Hamiltonian, we calculate its derivative function:

$$\frac{\partial H}{\partial f_{PTO}} = \frac{1}{m+a_\infty}\left(-p_2 + \dot{z}\left[1 - b'\left(\frac{\dot{z}\cdot f_{PTO}}{P_{max}}\right)\right] - 2\cdot\tilde{c}_{loss}\cdot f_{PTO}\right) \tag{34}$$

With the information given by the derivative of the barrier function, we can rewrite this expression:

$$\frac{\partial H}{\partial f_{PTO}} = \frac{1}{m+a_\infty}\left(-p_2 + \dot{z} - |\dot{z}|b'\left(\frac{|\dot{z}|\cdot f_{PTO}}{P_{max}}\right) - 2\cdot\tilde{c}_{loss}\cdot f_{PTO}\right) \tag{35}$$

This function is strictly decreasing with respect to f_{PTO}, so there is only one global extremum, and it is always a maximum because the derivative function changes sign from positive to negative:

$$0 = -p_2 + \dot{z} - |\dot{z}|b'\left(\frac{|\dot{z}|\cdot f_{PTO}}{P_{max}}\right) - 2\cdot\tilde{c}_{loss}\cdot f_{PTO} \tag{36}$$

In this case, the sign of f_{PTO} is always the same as the sign of $(\dot{z}-p_2)$ because the function is strictly decreasing and y-intercept equals $(\dot{z}-p_2)$ (see Fig. 6).

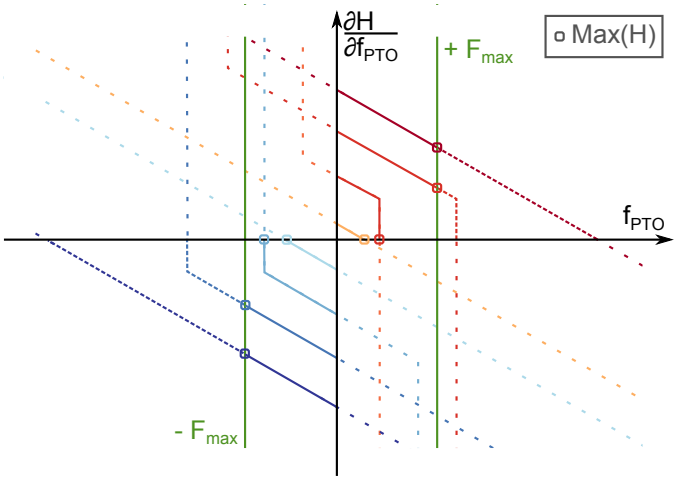

Fig. 6. Maximization of the Hamiltonian performed by the study of its derivative. Eight different cases are illustrated here according to the sign of $(\dot{z}-p_2)$, the influence of the barrier function for the passage by zero and if the passage by zero is in or out the admissible domain.

Three different cases exist, that depend on the mechanical power $f_{PTO}\cdot\dot{z}$:

- $|f_{PTO}\cdot\dot{z}| \leq (1-\epsilon)\cdot P_{max}$;
- $f_{PTO}\cdot\dot{z} > (1-\epsilon)\cdot P_{max}$;
- $f_{PTO}\cdot\dot{z} < -(1-\epsilon)\cdot P_{max}$;

And the respective solutions are:

- $f_{PTO} = \dfrac{\dot{z}-p_2}{2\cdot\tilde{c}_{loss}}$;
- $f_{PTO} = \dfrac{(\dot{z}-p_2)\cdot\epsilon^2 + \dot{z}\cdot(1-\epsilon)}{2\cdot\tilde{c}_{loss}\cdot P_{max}\cdot\epsilon^2+\dot{z}^2}P_{max} \approx \dfrac{P_{max}}{\dot{z}}$;
- $f_{PTO} = \dfrac{(\dot{z}-p_2)\cdot\epsilon^2 - \dot{z}\cdot(1-\epsilon)}{2\cdot\tilde{c}_{loss}\cdot P_{max}\cdot\epsilon^2+\dot{z}^2}P_{max} \approx -\dfrac{P_{max}}{\dot{z}}$;

Let's notice that the value of the parameter ϵ has no effect because of the simplification done in these solutions.

So, we consider the first case. If the result does not respect the condition, we use the second or the third case according to the sign of $(\dot{z}-p_2)$.

If the force f_{PTO} respects the force constraint, the problem is solved; if not, we know that the force constraint must be met. To maximize the Hamiltonian, we must use the following relation:

$$f_{PTO} = \text{sign}\left(\frac{\partial H}{\partial f_{PTO}}\right) F_{max} \tag{37}$$

We have already seen that the derivative of the Hamiltonian has only one sign change, and it is outside the control interval in this case. So the sign of the derivative in the control interval is the same (see Fig. 6), and in particular:

$$\text{sign}\left(\frac{\partial H}{\partial f_{PTO}}\right) = \text{sign}\left(\frac{\partial H}{\partial f_{PTO}}\left(f_{PTO}=0\right)\right) \tag{38}$$

$$= \text{sign}\left(\dot{z} - p_2\right) \tag{39}$$

So, we finally have:

$$f_{PTO} = \text{sign}\left(\dot{z} - p_2\right) F_{max} \tag{40}$$

The complete algorithm to find the optimal f_{PTO} as a function of the state vector x and the costate vector p is illustrated in Fig. 7.

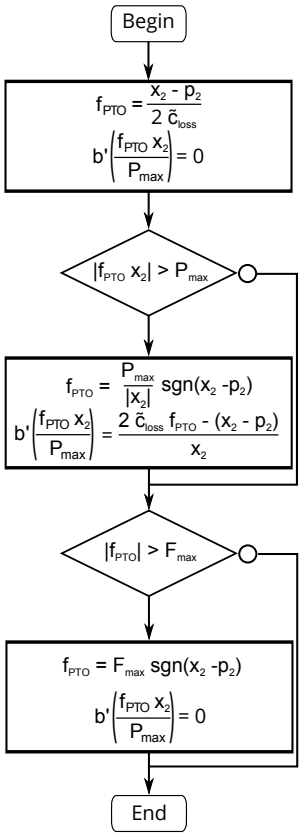

Fig. 7. Algorithm used to maximize the Hamiltonian as a function of the state vector x and the costate vector p.

E. MPC resolution

A standard multiple shooting method [18] was used to solve this MPC problem. We can sum up the dynamic and the control relations with these three equations:

$$\dot{x} = \frac{\partial H}{\partial p}(t, x, p, u) \tag{41}$$

$$\dot{p} = -\frac{\partial H}{\partial x}(t, x, p, u) \tag{42}$$

$$u = f_{PTO}(x, p) \tag{43}$$

If we rewrite these relations with $z = \begin{bmatrix} x & p \end{bmatrix}^T$, we can have:

$$\dot{z} = \begin{bmatrix} \frac{\partial H}{\partial p}(t, z, f_{PTO}(z)) \\ -\frac{\partial H}{\partial x}(t, z, f_{PTO}(z)) \end{bmatrix} = F(t, z) \tag{44}$$

With the simple shooting method, we want to find $z_{sol}(t_0)$ in such a way that the two boundaries conditions are met:

$$x_{sol}(t_0) = x(t_0) \tag{45}$$

$$p_{sol}(t_0 + T_h) = \frac{1}{m + a_\infty} \cdot \alpha \cdot 2\ P\ x(t_0 + T_h) \tag{46}$$

Compared to the simple method of shooting, multiple shooting method consists of cutting the interval into N intervals, and searching the z values at the beginning of each sub-interval. We must take into account matching conditions between the sub-intervals.

We improve the stability of the method by increasing the number of nodes, but the problem becomes bigger. Indeed, each new node adds 12 new variables that need to be found (6 for the state and 6 for the costate). This is indeed the principle of the multiple shooting method, as opposed to the simple shooting method where the errors with respect to the initial condition increase exponentially with the horizon size T_h.

With the multiple shooting method, we want to find, for example, $z_{sol1}(t_0)$ and $z_{sol2}(t_0 + T_h/2)$ such as:

$$x_{sol1}(t_0) = x(t_0) \tag{47}$$

$$z_{sol1}(t_0 + T_h/2) = z_{sol2}(t_0 + T_h/2) \tag{48}$$

$$p_{sol2}(t_0 + T_h) = \frac{1}{m + a_\infty} \cdot \alpha \cdot 2\ P\ x(t_0 + T_h) \tag{49}$$

The problem has been subdivided by two in this example but it can be subdivided by more than two.

To solve this problem, we use the Maltab function *fsolve()*.

IV. Results

The MPC control described in III has been simulated with the buoy model. Each 0.5 s, the optimal control is used to compute the costate vector in order to decide the next PTO force to be applied in the next 0.5 s. We have considered this time to be short enough for the control performances, but the sampling time used in the MPC algorithm is still 0.1 s. It seems that it is possible to obtain real-time computing with numerical optimization and the use of correct technology (like Digital Signal Processors or Field-Programmable Gate Arrays). Indeed, it takes around 0.5 s for reasonable time horizon to compute the control with an Intel-Xeon X5550 clocked at 2.67 GHz. Table II gives the default parameters

used in this study: if no further information is given, these parameters are used. Each simulation has a duration of 250 s in order to model one sea state.

TABLE II
MODEL PREDICTIVE CONTROL DEFAULT PARAMETERS

Maximum PTO force	F_{max}	1 MN
Maximum PTO power	P_{max}	1 MW
Loss coefficient	c_{loss}	0.1 MW/MN^2
Control loss coefficient	$\tilde{c}_{loss}$	0.1 MW/MN^2
Time horizon	T_h	12 s
Weight of the final state energy	α	0.5

Fig. 8 illustrates for one sea state ($H_s = 2\,\text{m}$, $T_p = 8\,\text{s}$) two different types of control: an optimized passive control with the PTO force proportional to the speed and the MPC results. We can verify that the force and the power constraints are respected, while the PTO force is much more continuous than typical bang-bang controls [19]. The average production for the passive control is 45 kW and 110 kW for the MPC, that is around two times more.

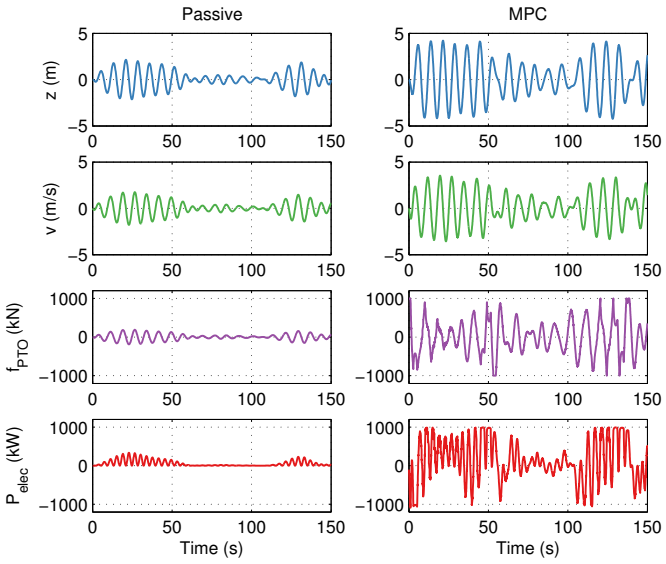

Fig. 8. Comparison between an optimized passive control and the Model Predictive Control (sea state: $H_s = 2\,\text{m}$, $T_p = 8\,\text{s}$ with the same excitation profile)

A. Influence of the time horizon and the weight of the final mechanical energy

Two parameters have a huge influence on the control performance: the time horizon T_h and the weight of final state mechanical energy α. We can predict that the performance is globally increasing with the time horizon, because we use a perfect prediction of the excitation. This is what we observe in figure 9.

The influence of the coefficient α must be lower for a bigger horizon T_h, because this energy become smaller compared to the converted energy. We can also observe this in figure 9.

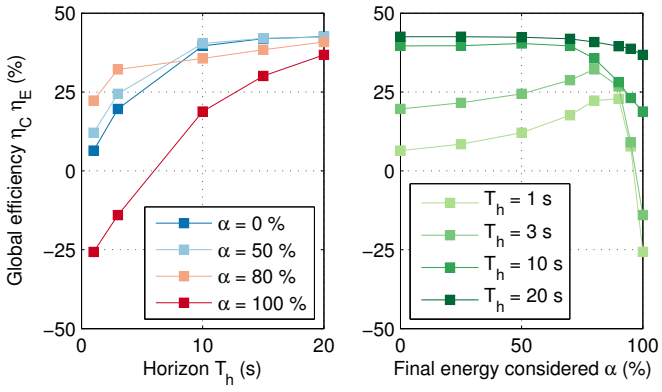

Fig. 9. Control performance for different time horizon T_h and weight of final state mechanical energy α (sea state: $H_s = 3\,\text{m}$, $T_p = 9\,\text{s}$ with the same excitation)

We can deduce from figure 9 that, for each time horizon T_h, there exists an optimal value of α between 0 and 100 % that maximize the performance of the control, that is the electrical energy converted. This optimum is smaller with larger time horizon and its limit seems to be 0.

Others MPC controls for wave energy converters do not take into account the final state energy (that correspond to the case $\alpha = 0$): we can see an important benefit with this additional setting parameter, in particular with small time horizon value. That could be very important if the numerical complexity or the prediction quality does not allow to have long time horizon.

But we see also that taking into account all the final state energy ($\alpha = 1$) is never the best way to maximize the performance, because this mechanical energy have less value than converted energy: we can even see that, for small time horizon, the wave energy converter consumes more energy than it produces.

B. Influence of the sea state

The performance of the control is different for each sea state, depending on how far the peak period of the excitation is from the natural resonant period of the system without control (here, around 7.2 s) and how powerful the sea state is (because a calm sea state needs less PTO force to have a good control efficiency). We can notice in figure 10 that the global efficiency is higher for relatively calm sea state and a peak period close to the natural resonant period.

We can notice that the shape of the global efficiency as a function of the time horizon is similar for all sea states, but it would no longer be the case with a real prediction of the excitation force.

C. Influence of an error and the electrical losses model

Apart from taking into account the final state energy in the MPC control, a second originality is to take into account a simplified loss model for the electrical chain. So it is

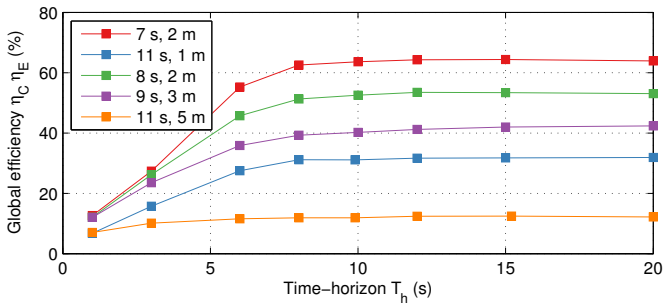

Fig. 10. Harvesting performance versus time horizon T_h for different sea states

important to evaluate what has been added with this additional information by a sensitivity study, illustrated by the figure 11: the hypothesis about the electrical chain is the same ($c_{loss} = 0.1\,\text{MW/MN}^2$) but we change the coefficient use for the control ($\tilde{c}_{loss}$ from 0.01 to $1\,\text{MW/MN}^2$).

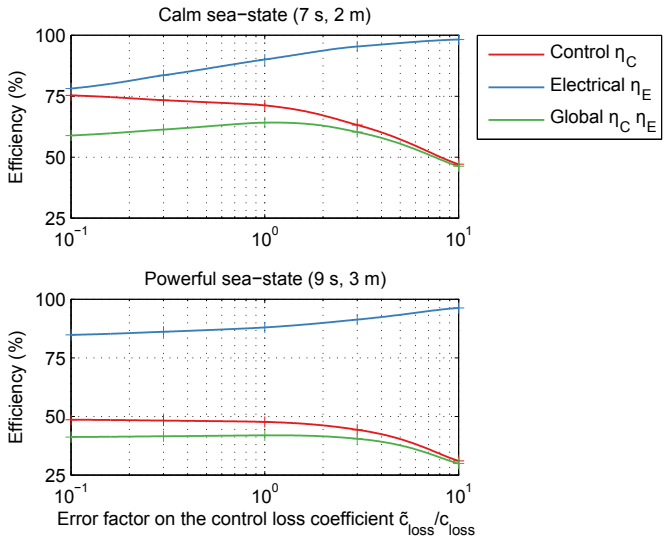

Fig. 11. Control efficiency, electrical efficiency and global efficiency with the same hypothesis but an error on the loss coefficient

We can predict that the control efficiency will be higher and the electric efficiency will be smaller for a smaller value of $\tilde{c}_{loss}$. The maximum value of the global efficiency must correspond to $\tilde{c}_{loss} = c_{loss} = 0.1\,\text{MW/MN}^2$. This corresponds to the results show in figure 11. We can notice that an important error on the loss model (by a factor 10) has perceptible impact on global efficiency, but it is not the case for a smaller error (by a factor 3), that could still be considered as an important error. Our MPC seems quite robust against a modelling error in the loss coefficient.

We can notice that it is more important to take into account losses for calm sea state, because the control efficiency for powerful sea states is already limited by the maximum force and the maximum power for powerful sea states.

D. Pre-sizing of the electrical chain

One important decision to be made for the design of a Wave Energy Converter is the size of its Power Take-Off. Here we investigate the influence of maximum force and maximum power on the global efficiency of the conversion, but also on the total profitability (that is the reduction of the per-kWh cost). Indeed, a bigger Power take-Off allows directly a more efficient conversion, but with a bigger cost, that is not always the best way for the global per-kWh cost.

The total energy produced during the lifetime of a Direct Wave Energy Converter E_{Prod} correspond to a 8 years case with the sea state (9 s, 3 m), hypothetically equivalent to 20 years in Yeu's island site [20]. We can see the increase of E_{Prod} with the maximum force and the maximum power in the first subfigure (Buoy profitability) of figure 12.

The second and the third subfigures of figure 12 (static and electro-mechanical converter profitability) correspond respectively to the ratio between the energy produced during its lifetime by the WEC E_{Prod} and the maximum power (for the static converter profitability) or the maximum force (for the electro-mechanical converter profitability). Indeed, we use the assumption that the maximum power depends mainly on the static converter size and the maximum force on the electro-mechanical converter (machine) size.

We deduce a cost per-kWh C_{kWh} with the following hypotheses:

- Static converter cost C_P: 100 k€/MW ;
- Electro-mechanical converter cost C_F: 200 k€/MN ;
- Cost of the installed DWEC without the electrical chain C_B: 2000 k€.

So we can calculated C_{kWh} with the following relation:

$$C_{kWh} = \frac{C_B + C_P\ P_{Max} + C_F\ F_{Max}}{E_{Prod}} \tag{50}$$

The last figure (Total profitability) correspond to the inverse of this value. We can cite the French WEC feed-in tariff for comparison, that corresponds to 6.7 kWh/€. According to this study, an electrical chain with a 2 MW converter and a 2 MN electrical machine has a smaller per-kWh cost than smaller electrical chain.

V. Conclusion

This paper proposes an enhanced Model Predictive Control for a Wave Energy Converter (in this case, a heaving buoy): this model takes into account an original energetic model and the main constraints of an electrical chain (limitation in force, in power and losses depending on Power Take-Off force).

The mixed constraint on the power is taken into account with a barrier function, in order to use the maximum Pontryagin's principle. A classical multishooting method is used to compute the optimal control.

The results of the control are consistent with most intuitions. The control is close of its maximum performance from 12 s time horizon (the natural resonant period of the system is 7.2 s). Considering final state energy in the control allows better performance for shorter time horizon, that could be

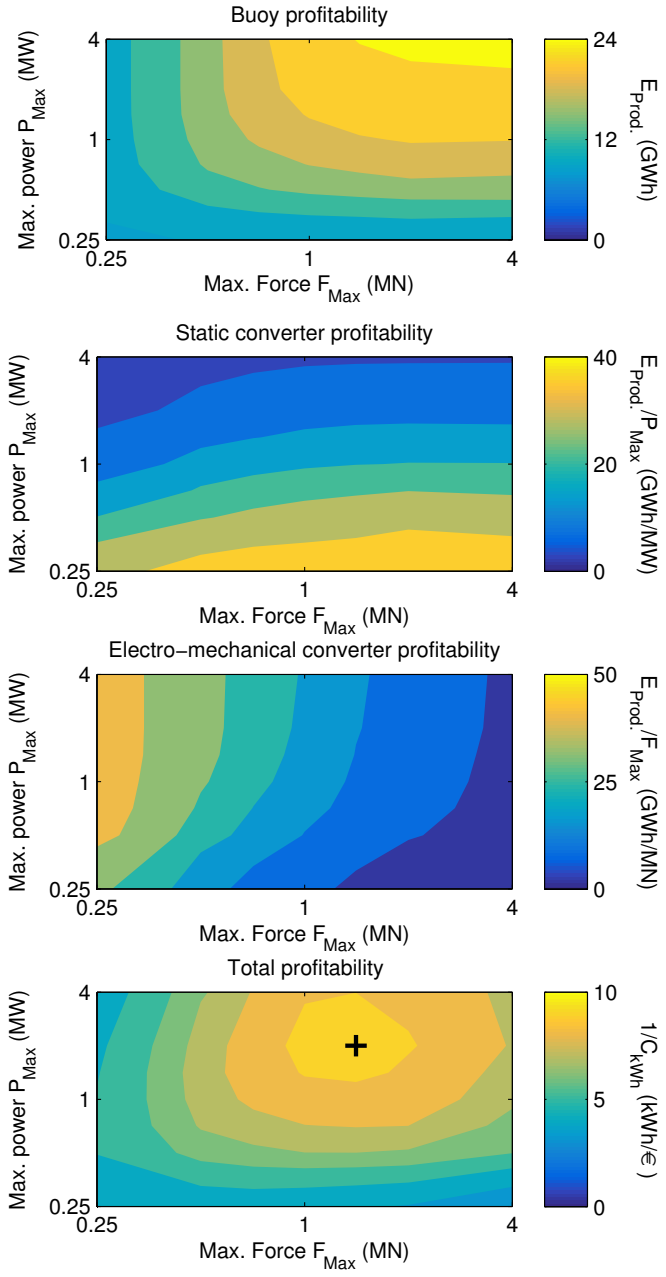

Fig. 12. Pre-sizing of the electrical chain: profitability of different element of the WEC as a function of the maximum force and maximum power

important if there are numerical or prediction issues (here, a perfect prediction is used).

We notice that it is more important for the global efficiency to take into account losses for calm sea state, because maximum force and maximum power limit already the control efficiency.

The end of the study has focused on presizing optimization for a Direct Wave Energy Converter, in a global context of kWh cost minimization. Electrical chain losses and force or power amplitude constraints play an important role in designing the electric chain, and hence in its cost. Moreover, they play a key role in the conversion mechanism. For this reason, the control strategy and the electric chain design are highly correlated. We use here a simplified economic model in order to optimize the size of the electrical chain (maximum force that correspond to the electro-mechanical converter and maximum power that correspond to the static converter).

The MPC seems to be a good solution to optimize the harvesting and respect the main constraints due to the use of an electrical chain. Future works could compare it with other control strategy. However, in order to do a fair comparison, these controls must use realistic observations and predictions. Besides the conversion efficiency, other relevant issues must also be compared, as stability, practical feasibility, flexibility and robustness. These are particularly important in the harsh sea environment. Moreover, a better control strategy could lead to other WEC designs, that could also be studied.

This study is part of a more general design analysis of a complete electric conversion chain that takes lifetime into account [9]. We can notice that the power fluctuations are more stringent with optimal control compared to passive one. This could lead to premature aging of the electrical chain (in particular the converter [21]) or grid integration issue (in particular the need to smooth the production with a flicker contraint [22]).

ACKNOWLEDGMENT

This work has been supported by the French National Research Agency (ANR) within the scope of the project QUALIPHE (power quality and grid integration of Direct Wave Energy Converters), which is part of the PROGELEC program.

REFERENCES

[1] J. Cretel, G. Lightbody, G. Thomas, and A. Lewis, "Maximisation of Energy Capture by a Wave Energy Point Absorber using Model Predictive Control," in *Eighteenth IFAC World Congress*, Milan, 2011, pp. 3714–3721.

[2] J. V. Ringwood, G. Bacelli, and F. Fusco, "Energy-Maximizing Control of Wave-Energy Converters: The Development of Control System Technology to Optimize Their Operation," *Control Systems Magazine, IEEE*, vol. 34, no. 5, pp. 30–55, Sep. 2014.

[3] F. Fusco and J. Ringwood, "Robust Control of Wave Energy Converters," in *Control Applications, IEEE International Conference on*, Antibes (France), 2014, pp. 292–297.

[4] J. Sjolte, G. Tjensvoll, and M. Molinas, "Self-sustained all-electric wave energy converter system," *International Journal for Computation and Mathematics in Electrical and Electronic Engineering*, vol. 33, no. 5, pp. 1705–1721, 2014.

[5] A. De le Villa Jaen, A. García-Santana, and D. E. Montoya-Andrade, "Maximizing output power of linear generators for wave energy conversion," *Electrical Energy Systems, International Transactions on*, 2013.

[6] R. Genest, F. Bonnefoy, A. H. Clément, and A. Babarit, "Effect of non-ideal power take-off on the energy absorption of a reactively controlled one degree of freedom wave energy converter," *Applied Ocean Research*, vol. 48, pp. 236–243, Oct. 2014.

[7] E. Tedeschi and M. Molinas, "Tunable Control Strategy for Wave Energy Converters With Limited Power Takeoff Rating," *Industrial Electronics, IEEE Transactions on*, vol. 59, no. 10, pp. 3838–3846, Oct. 2012.

[8] G. Li and M. R. Belmont, "Model predictive control of sea wave energy converters Part I: A convex approach for the case of a single device," *Renewable Energy*, vol. 69, pp. 453–463, Sep. 2014.

[9] J. Aubry, H. Ben Ahmed, and B. Multon, "Sizing Optimization Methodology of a Surface Permanent Magnet Machine-Converter System over a Torque-Speed Operating Profile : Application to a Wave Energy Converter," *Industrial Electronics, IEEE Transactions on*, vol. 59, no. 5, pp. 2116,2125, 2012.

[10] J. Sjolte, C. Sandvik, E. Tedeschi, and M. Molinas, "Exploring the Potential for Increased Production from the Wave Energy Converter Lifesaver by Reactive Control," *Energies*, vol. 6, no. 8, pp. 3706–3733, Jul. 2013.

[11] T. Kovaltchouk, B. Multon, H. Ben Ahmed, F. Rongère, A. Glumineau, and J. Aubry, "Influence of control strategy on the global efficiency of a Direct Wave Energy Converter with electric Power Take-Off," in *Ecological Vehicles and Renewable Energies (EVER)*, Monte-Carlo, Monaco, Mar. 2013, pp. 1–10.

[12] G. Delhommeau, "Seakeeping codes aquadyn and aquaplus," *Proc. of the 19th WEGEMT school, numerical simulation of hydrodynamics: ships and offshore structures*, 1993.

[13] J. N. Newman, *Marine hydrodynamics*. MIT press, 1977.

[14] A. H. Clément and A. Babarit, "Discrete control of resonant wave energy devices." *Philosophical transactions. Series A, Mathematical, physical, and engineering sciences*, vol. 370, no. 1959, pp. 288–314, Jan. 2012.

[15] "CVX: Matlab Software for Disciplined Convex Programming." [Online]. Available: http://cvxr.com/cvx/

[16] J. Macki and A. Strauss, *Introduction to Optimal Control Theory*. Springer New York, 1982.

[17] M. De Pinho, R. Vinter, and H. Zheng, "A maximum principle for optimal control problems with mixed constraints," *IMA Journal of Mathematical Control and Information*, vol. 18, pp. 189–205, 2001.

[18] M. Diehl, H. G. Bock, H. Diedam, and P.-B. Wieber, "Fast direct multiple shooting algorithms for optimal robot control," in *Fast Motions in Biomechanics and Robotics*, vol. 340, Heidelberg, Germany, 2005, pp. 65–93.

[19] E. Abraham and E. C. Kerrigan, "Optimal active control of a wave energy converter," in *Decision and Control (CDC), 2012 IEEE 51st Annual Conference on*. Maui (USA): Ieee, Dec. 2012, pp. 2415–2420. [Online]. Available: http://ieeexplore.ieee.org/lpdocs/epic03/wrapper.htm?arnumber=6426993

[20] A. Babarit, H. Ben Ahmed, A. H. Clément, V. Debusschere, G. Duclos, B. Multon, and G. Robin, "Simulation of electricity supply of an Atlantic island by offshore wind turbines and wave energy converters associated with a medium scale local energy storage," *Renewable Energy*, vol. 31, no. 2, pp. 153–160, Feb. 2006. [Online]. Available: http://linkinghub.elsevier.com/retrieve/pii/S0960148105002223

[21] T. Kovaltchouk, J. Aubry, B. Multon, and H. Ben Ahmed, "Influence of IGBT current rating on the thermal cycling lifetime of a power electronic active rectifier in a direct wave energy converter," in *Power Electronics and Applications (EPE)*, Lille, 2013, pp. 1–10.

[22] T. Kovaltchouk, B. Multon, H. Ben Ahmed, J. Aubry, and P. Venet, "Enhanced Aging Model for Supercapacitors Taking Into Account Power Cycling : Application to the Sizing of an Energy Storage System in a Direct Wave Energy Converter," *Industry Applications, IEEE Transactions on*, vol. 51, no. 3, pp. 2405–2414, 2015.